Smart Materials and Structures 2005, Vol. 14, No. 1, pp170-176

Ultrasonic sensing using Yb^{3+}/Er^{3+}-codoped distributed feedback fibre grating lasers

C-C. Ye* and R. P. Tatam

Optical Sensors Group, Centre for Photonics and Optical Engineering,

School of Engineering, Cranfield University,

Cranfield, Bedford MK43 0AL, UK

Tel: +44-1234-754630, Fax: +44-1234-752452, Email: r.p.tatam@cranfield.ac.uk

*C-C Ye's current address: Department of Electronic Engineering, School of Computer & Information Engineering, Xiamen University, Xiamen, China

Abstract

Yb^{3+}/Er^{3+}-codoped distributed feedback (YbEr-DFB) fibre grating lasers have been investigated for the detection of ultrasonic Lamb waves generated in an aluminum plate. Two sensor configurations have been investigated. A path length imbalanced readout Mach-Zehnder interferometer was used to measure the laser frequency shift induced by ultrasonic vibration. The resolution to out-of-plane displacement was 3 $x10^{-15}$ m/√Hz for a continuous ultrasonic wave at a frequency of 470 kHz. Ultrasonic waves were also detected by directly monitoring the laser output power. This simplified configuration is useful for tone burst AE signals generated by a low energy impact.

Short title: Ultrasonic sensing using DFB fibre lasers

Keywords:

Ultrasonic sensing, distributed feedback fibre laser, fibre Bragg grating, Yb^{3+}/Er^{3+}-codoped fibre

PACS classification numbers:

42.81.Pa, Sensors;

07.60.Vg, Fiber-optic instruments.

42.55.Wd, fiber lasers

43.58.+z, Acoustical measurements and instrumentation

43.40.Le, Techniques for nondestructive evaluation and monitoring, acoustic emission

Ultrasonic sensing using Yb^{3+}/Er^{3+}-codoped distributed feedback fibre grating lasers

C-C. Ye and R. P. Tatam
Optical Sensors Group, Centre for Photonics and Optical Engineering,
School of Engineering, Cranfield University,
Cranfield, Bedford MK43 0AL, UK
Tel: +44-1234-754630, Fax: +44-1234-752452, Email: r.p.tatam@cranfield.ac.uk
*C-C Ye's current address: Department of Electronic Engineering, School of Computer & Information Engineering, Xiamen University, Xiamen, China

1. Introduction

Structural impact or fracture events are associated with the generation of acoustic stress waves, typically in a frequency range between 100 kHz and a few MHz. Acoustic-emission (AE) detection has been established as one of the main non-destructive testing techniques for monitoring structural health and integrity [1-4]. For airframe and large civil structures in particular, the monitoring of impacts and damage using the AE detection method is important for safety and cost reduction [1, 4]. Fibre Bragg grating (FBG) strain sensors have considerable advantages over conventional piezoelectric sensors, such as immunity to electromagnetic interference, ease of installation and multiplexing capability. Different techniques employing FBGs to detect AE have been demonstrated [2-7]. A minimum detectable dynamic strain in the order of 10 nanostrain has been demonstrated for sensors using passive FBGs [3, 4]. Higher strain sensitivity at a few 100 Hz was obtained using a pi-phase shifted FBG which was interrogated with a tuneable laser [7]. The maximum measurable AE frequency using this technique is limited by the frequency scanning speed of the tuneable laser.

AE detection using fibre grating lasers offers not only the advantages associated with FBG sensors, but also the potential to measure AE signals with much higher sensitivities than FBG sensors [8-12]. The linewidth of fibre lasers is typically a few tens of kHz, corresponding to a coherence length of the order of tens of km. In this sensor configuration, the AE signals

perturb the laser cavity thus modulating the lasing frequency which can be measured using a path length imbalanced readout Mach-Zehnder interferometer (MZI). Since the laser linewidth is narrow, a long path length can be used and high AE sensitivity can be realised. For example, an axial strain sensitivity of 10^{-14} /√Hz at 7 kHz using a single mode distributed Bragg reflector (DBR) Er^{3+}-doped fibre laser has been reported [8]. Distributed feedback (DFB) fibre grating lasers provide more robust single frequency operation without mode-hopping [13], and are expected to offer better performance for AE sensing. The high acoustic sensitivity also provides the possibility of using DFB fibre lasers as compact optical fibre hydrophones in sonar applications [10-12].

We have observed that the output power of a DFB fibre laser is sensitive to ultrasonic waves that impinge on the laser cavity, in particular when the vibration frequencies are close to the relaxation oscillation frequency of the laser [14]. A weak AE signal either initiates a relaxation oscillation of the laser, or modulates the laser output power with the same frequency as the AE signal. Therefore, the ultrasonic waves can be detected by directly monitoring the laser output power.

In this paper we report the development of AE sensors based on Yb^{3+}/Er^{3+}-codoped DFB (YbEr-DFB) fibre grating lasers. The response of the fibre laser to ultrasonic Lamb waves generated in a 3-mm thick aluminium plate has been investigated. Two sensor configurations have been investigated. (1), a path length imbalanced readout Mach-Zehnder interferometer was used to measure the laser frequency shift induced by ultrasonic vibration. (2), the detection of ultrasonic waves by directly monitoring the laser output power.

2. YbEr-DFB fibre grating laser

Figure 1 shows a schematic of the YbEr-DFB fibre laser deployed for AE detection. The laser head was a phase-shifted FBG written into an Yb^{3+}/Er^{3+}-codoped fibre (Koheras, C15). The length of the grating was 5 cm, and was recoated with polyimide to a diameter of 155 μm. Standard telecommunication fibre was spliced to one or both sides of the doped fibre, approximately 5 mm from the grating ends. A 977 nm fibre pigtailed solid state pump laser was coupled into the Yb^{3+}/Er^{3+}-codoped fibre through a 980/1550 nm fibre wavelength division multiplexer (WDM). Two YbEr-DFB fibre lasers were investigated, operating at wavelengths of 1549.7 (YbEr-DFB-1) and 1548.0 (YbEr-DFB-2) nm. The laser output was

separated from the pump light through the WDM and was measured after a polarisation-insensitive optical fibre isolator FI-1.

Part of the fibre containing the phase-shifted FBG must be placed on a heat sink to dissipate the heat from the self-heating due to pump laser absorption. The laser output was monitored using a scanning Fabry-Perot interferometer with 80 MHz resolution. The laser was observed to lase on two orthogonally polarised modes, separated by approximately 1.49 GHz. When the fibre of the first laser YbEr-DFB-1 was twisted by approximately 180^{o} over the 10 cm long fibre section containing the phase-shifted FBG, the laser operated in a single polarisation mode [15]. Using the delayed self-heterodyne method [16] with a 2 km fibre delay line, the linewidth of the laser was measured to be 100 kHz, limited by the measurement resolution.

Single polarisation mode operation was also achieved by separating part of laser YbEr-DFB-2 from the heat sink and not twisting the fibre. A possible reason for this is that the non-uniform distribution of temperature along the fibre made the lasing conditions more favourable for one of the orthogonally polarised modes than the other. It is beyond the scope of this paper to discuss the laser mechanisms in more detail.

The measured laser output powers and relative intensity noise spectra are shown in Figure 2. The noise spectra recorded using a RF spectrum analyser with a bandwidth of 3 kHz for different pump powers are shown in Figure 2(a). The background noise spectrum of the photoreceiver (P_p=0) was recorded when the pump laser was turned off. The laser relaxation oscillation frequency increases as the pump power increases. In Figure 2 (b), the peak frequency of relaxation oscillation and laser power output from the isolator FI-1 are plotted against pump power for the two lasers. The threshold pump power was less than 10 mW. The single frequency laser power was greater than 0.5 mW and 1.0 mW respectively for the two lasers for 20 mW of pump power, demonstrating that YbEr-DFB fibre lasers are more efficient than DFB fibre lasers using Er^{3+}-doped fibre. Such a high power signal source is an advantage for constructing the sensor system for high frequency measurement as the photoreceiver amplifier can be optimised for high frequency without the requirement for high gain.

3. AE sensing experiment

Figure 3 shows the configuration of the AE sensing experiment using an YbEr-DFB fibre laser. An YbEr-DFB laser was placed on an aluminium plate, that was 3 mm thick and with lateral dimensions of 50x50 cm^2.

3.1. Generation of ultrasonic lamb waves in an aluminium plate

Ultrasonic waves were generated by a piezoelectric pressure transducer (PA-g) (Physical Acoustics, model: WD), which was driven directly by a synthesized function generator without using an RF amplifier. The vibration was coupled to the aluminium plate using a perspex wedge with the wedge angle approximately equal to the critical angle for the interface between perspex and aluminium ($\theta = 25^o$), so that shear waves propagation is dominant in the aluminium plate [17]. In general the ultrasonic waves generated interact in a complex manner with the laser sensor. To simplify interpretation of the signals, the vibration frequency was kept below 500 kHz, so that the frequency-thickness product is smaller than 1.5 MHz·mm and the ultrasonic wave in the aluminium plate could be approximately treated as a zero order mode Lamb wave, i.e. antisymmetric mode A_0 and symmetric mode S_0 [17].

3.2. Coupling of vibration from the aluminium plate to the laser

When the ultrasonic vibration was generated in the aluminium plate, the laser frequency shift and power change results from the vibration-induced perturbations in the laser cavity. In our preliminary experiments [14], the entire length of YbEr-DFB laser was placed on an aluminium plate using two pieces of 5 mm wide tape. However, the laser also responds when only part of the laser is exposed to the ultrasonic vibration. This allows high spatial resolution sensing. As shown in Figure 1, a layer of lens tissue was used as the AE isolation layer. The 3 mm long sensing element of the DFB laser was covered by a layer of lens tissue and held on the plate using a piece of tape. Vacuum grease was used to improve the coupling between the fibre and the aluminium plate surface.

3.3. Measurement of Lamb wave induced laser frequency shift

The laser output was divided into two using a 50:50 fibre coupler after the fibre isolator FI-1. A path length imbalanced readout MZI was used to measure the laser frequency shift induced by ultrasonic vibration. The optical path difference (OPD) of the MZI was 125 m. An acousto-optic modulator (AOM) was connected in one of the MZI arms to introduce a frequency shift of 34.98 MHz and enable heterodyne signal processing. A polarization controller was used to

ensure that the polarization states in the two arms were matched. The two outputs from the MZI were detected using a balanced photoreceiver, and then processed by either a 100MHz 8-bit digitising card and computer, or a digital oscilloscope / RF spectrum analyzer. The use of a balanced photoreceiver minimises the laser power modulation signal when the two outputs of the MZI are approximately equal. The laser output from the second port of fibre coupler C1 was simultaneously monitored using a scanning Fabry-Perot interferometer.

A second piezoelectric pressure transducer (PA-s) positioned 10 mm from the centre of the YbEr-DFB laser was used to detect the Lamb waves, providing an independent measurement for the Lamb waves at the approximate location of the DFB laser. The output signal from PA-s was amplified by a pre-amplifier (A1), then by the amplifier (A2). PA-s and PA-g were the same type of pressure transducers. Vacuum grease was used to improve the coupling between the piezoelectric transducers and the aluminium plate surface.

Figure 4 shows the phase spectrum of the fibre laser recorded from the output of MZI using a spectrum analyser. The first peak at frequency f_0=34.98 MHz resulted from the AOM. The lower peak at (f_0 + 320) kHz corresponds to the laser noise. The peak at (f_0 + 470) kHz appeared when the vibration at 470 kHz was generated in the aluminium plate.

In order to estimate the laser sensitivity to the Lamb waves, it is appropriate to assume that the out-of-plane displacement was dominant on the surface for the test signal at 470 kHz. This approximation was made since the amplitude ratio of the out-of plane displacement to the in-plane displacement of the A_0 mode on the surface of a 3 mm thick aluminium plate was approximately 1.5, and the ratio of the out-of plane displacement of the A_0 mode to the in-plane displacement of the S_0 mode was approximately 6 [17]. In addition, since the fibre was not bonded to the plate, the coupling coefficient for in-plane-displacement between the fibre and the plate must be lower than that for out-of-plane displacement.

The out-of plane displacement on the plate surface associated with the test ultrasonic wave propagating in the aluminium plate was approximately $3\text{x}10^{-11}$ m, based on measurements using a single point laser Doppler vibrometer (Polytec, OFV-3001/303/OVD-02). The minimum detectable velocity was 0.5 μm/s, corresponding to a displacement of $2\text{x}10^{-13}$ m at

470 kHz. The minimum detectable out-of plane displacement measured using fibre laser was $1.5x10^{-13}$ m, corresponding to a resolution of $3x10^{-15}$ m/√Hz.

3.4. Measurement of Lamb wave induced laser power modulation

The laser output power was found to respond directly to the ultrasonic Lamb waves. Figure 5 shows the response of the YbEr-DFB laser and PA-s sensor to the ultrasonic waves generated by the piezoelectric transducer, PA-g. The voltage applied to PA-g was a sine wave at 250 kHz (Figure 3(a)). The output from PA-s and from the YbEr-DFB-2 laser are shown in Figure 5 (b) and (c) respectively. The output power of the laser is modulated at the same frequency as that of the ultrasonic wave. The laser power variation possibly results from the vibration induced perturbation of the value of the phase shift constant of the DFB laser. Quantifying this result with the underlying physics is the subject of further research.

3.4.1. Effects of pump power

The vibration induced laser power modulation was observed to be strongly frequency dependent. Since the vibration amplitude of the transducer, the vibration coupling loss from the transducer to the aluminium plate and the properties of Lamb waves in the plate depend strongly on frequency, it is complex to measure the vibration amplitude coupled to the laser as a function of frequency. The operation state of the YbEr-DFB laser itself has a strong effect on its response to ultrasonic waves. Since the laser relaxation oscillation frequency increases as the pump power increases, the laser sensitivity will be different for the same test vibration signal if the pump power is varied. Therefore, the laser output power was measured for different pump powers at the same ultrasonic frequency.

When an ultrasonic wave at 340 kHz was generated in the plate, the relative intensity noise spectrum of YbEr-DFB-2 was measured for different pump powers using an RF spectrum analyser. The voltage amplitude applied to the transducer PA-g was 5 V. Figure 6 shows the measured spectrum for a pump power of 23 mW. The peak frequency of relaxation oscillation, fr, was 476 kHz. The peak at 340 kHz results from the laser response to the test ultrasonic wave. The signal to noise ratio (S/N) at the test frequency was 27 dB, which can be used as the characteristic sensitivity of the laser to the ultrasonic wave. In figure 7, the measured S/N at 340 kHz is plotted against peak relaxation oscillation frequency, fr, which increased with pump power. The S/N increased as fr increased. With such laser sensitivity dependency on

pump power, the laser sensor can be tuned to optimise the measurement of vibrations in a specified frequency range.

3.4.2. Laser response to a tone burst

The DFB fibre laser can be used to monitor the transient AE signals on the surface of the aluminium plate. Figure 8 shows the response to a 5-cycle sine tone burst at 250 kHz. PA-g was 18 cm away from the centre of the DFB sensing section.

The group velocities of A_0 and S_0 modes at 250 kHz in an aluminium plate are 3.0 km/s and 5.3 km/s respectively [17]. The approximate 51 μs delay before either PA-s or the fibre laser responds to the tone burst corresponds to the time taken for the A_0 mode to propagate to the sensors. The size and shape of the sensing area for each sensor type are very different. The optical fibre has a cylindrical shape and therefore very little is in direct contact with the surface of the plate and has an interaction area at least two orders of magnitude less than the piezoelectric sensor (approximately $1mm^2$ compared to $250mm^2$). It is therefore probable that although the response of the two sensor types will be similar in form they will differ in detail. From these results it appears that the laser sensor has comparable sensitivity to the piezoelectric device, but when normalised for sensing area the fibre laser has much higher sensitivity. This issue will be the subject of future investigation.

3.4.3. Low energy impact detection

The laser response to impacts generated by dropping a steel ball is shown in Figure 9. The ball of 4.7 mm diameter and 0.43 g in weight was dropped from a height of 7 cm above the horizontal aluminium plate, corresponding to an initial impact energy of 0.3 mJ. The impact location on the plate was 15 cm from the centre of the YbEr-DFB-1 fibre laser on an aluminium plate of 13 x 50 x 0.3 cm^3. The subsequent bursts of laser power shown in Figure 9 resulted from the bouncing of the ball on the plate. The impacts occurring after the ball has bounced were weaker than the initial one, indicated by the smaller amplitude and shorter duration of the bursts of the laser power. Such a high sensitivity to impact could have applications in composite structures where the AE attenuation is very high.

4. Conclusions

YbEr-DFB fibre lasers have been used to detect ultrasonic Lamb waves generated in an aluminium plate. The vibration frequency was kept below 500 kHz, so that the ultrasonic wave in the 3 mm thick aluminium plate could be approximately treated as a zero order mode Lamb wave.

A path length imbalanced readout Mach-Zehnder interferometer was used to measure the laser frequency shift induced by ultrasonic vibration. The use of a balanced photoreceiver minimises the effects of laser power modulation. The out-of-plane displacement resolution was 3 $x10^{-15}$ m/√Hz for a continuous ultrasonic wave at a frequency of 470 kHz.

We have demonstrated that the output power of an YbEr-DFB fibre laser can be modulated by the ultrasonic waves generated in an aluminium plate, which has been exploited to develop an alternative method for AE sensing. By directly monitoring the laser power, the sensor system configuration has been considerably simplified. Since the laser sensitivity to the vibration depends on the pump power, the laser sensor can be tuned to suite the measurement of vibrations at a specified frequency range. This simplified configuration is useful for transient AE signals. The detection of low energy impacts has been demonstrated, indicating the potential for applications in composite structures where the AE attenuation is high.

Acknowledgements

This work was supported by the Engineering and Physical Sciences Research Council (EPSRC), UK and the Royal Society, UK. The laser Doppler vibrometer used in this work was provided by Lambda Photometrics Ltd.

References

1. Acoustic Emission: Standards and Technology Update, ed. Vahaviolos SJ, American Society for Testing and Materials: STP 1353 (1998)
2. Spillman WB, Claus RO 2002 Optical-fiber sensors for the detection of acoustic emission, MRS Bulletin, **27,** pp.396-9
3. Perez I, Cui HL, Udd E 2001 Acoustic emission detection using fiber Bragg gratings, Proc. SPIE, **4328**, pp. 209-15
4. Betz DC, Thursby G, Culshaw B and Staszewski WJ 2003 Acousto-ultrasonic sensing using fiber Bragg gratings, Smart Mater. & Struct. **12**, pp. 122-8

5. Takahashi N, Yoshimura K and Takahashi S 2000 Detection of ultrasonic mechanical vibration of a solid using fiber Bragg grating, Jpn. J. Appl. Phys. **39**, Part 1, No. 5B, pp.3134-8
6. Fisher NE, Webb DJ, Pannell CN, Jackson DA, Gavrilov LR, Hand JW, Zhang L, Bennion I 1998 Ultrasonic field and temperature sensor based on short in-fibre Bragg gratings, Electron. Lett. **34**, pp. 1139-40
7. Leblanc M, Kirkendall C, Dandridge A 2000 Acoustic sensing using free and transducer-mounted fiber Bragg gratings, Proc. OFS-14, pp. 592-5
8. Koo KP, Kersey AD 1995 Bragg grating-based laser sensors systems with interferometric interrogation and wavelength-division multiplexing, J. Lightwave Technol., **13**, pp.1243-9
9. Ronnekleiv E 2001 Frequency and intensity noise of single frequency fiber Bragg grating lasers, Optical Fiber Technology **7**, pp. 206-35
10. Lovseth SW, Kringlebotn JT, Ronnekleiv E, Blotekjaer K 1999 Fiber distributed-feedback lasers used as acoustic sensors in air, Appl. Optics **38**, pp.4821-30
11. Hill DJ, Nash PJ 2000 In-water acoustic response of a coated DFB fibre laser sensor, Proc. OFS-14, pp. 33-6
12. O'Neill SF, Webb DJ, Jackson DA, Zhang L, Bennion I 2000 Acoustic detection using erbium fibre Bragg grating lasers, Proc. OFS-14, pp.264-7
13. Loh WH, Samson BN, Dong L, Cowle GJ, Hsu K 1998 High performance single frequency fiber grating-based erbium: ytterbium-codoped fiber lasers, J Lightwave Technol. **16**, pp.114-8
14. Ye C-C and Tatam RP 2003 Acoustic-emission detection using Yb^{3+}/Er^{3+}-codoped fibre grating lasers, Proc. OFS-16, pp. 218-221
15. Haratjunian ZE, Loh WH, Laming RI, Payne DN 1996 Single polarisation twisted distributed feedback fibre laser, Electron. Lett. **32**, pp.346-8
16. Okoshi T, Kikuchi K, Nakayama A 1980 Novel method for high resolution measurement of laser output spectrum, Electron. Lett. **16**, pp.630-1
17. Rose JL 1996 Ultrasonic waves in solid media, Cambridge University Press

Captions

Figure 1 Schematic of the YbEr-DFB laser deployment

LD: 977nm laser diode

WDM: 980/1550nm wavelength division multiplexer

FI-1: polarisation-insensitive optical fibre isolator

Figure 2 (a) Laser relative intensity noise spectrum of YbEr-DFB-1 for different pump powers, (b) Frequency of relaxation oscillation (squares) and laser power (triangles) vs. pump power for the two YbEr-DFB lasers

Figure 3 Schematic of the fibre laser AE sensor.

FI-1, FI-2: polarisation-insensitive optical fibre isolators

FG: synthesized function generator

PA-g, PA-s: piezoelectric pressure transducers (Physical Acoustics, model: WD, ϕ18mm)

A1, A2: Physical Acoustics 1220A pre-amplifier and AE1A amplifier

F-P: scanning Fabry-Perot interferometer

C1, C2, C3: 1550nm 50:50 fibre couplers

AOM: acousto-optic modulator, PC: polarisation controller

WDM: 980/1550nm wavelength division multiplexer

Figure 4 Measured phase spectrum of the read out MZI.

The test signal was at 470 kHz, with out-of-plane displacement $\Delta X \approx 3 \times 10^{-11}$ m.

Bandwidth of spectrum analyser: 3 kHz

Figure 5 Response to the ultrasonic wave at 250 kHz generated by PA-g.

(a) Voltage applied to PA-g, (b) output from PA-s, and (c) laser YbEr-DFB-2

Figure 6 Laser relative intensity noise spectrum measured when an ultrasonic wave at 340 kHz was generated in the plate.

(YbEr-DFB-2, Bandwidth of the spectrum analyzer: 3 kHz)

Figure 7 The measured signal to noise ratio at 340 kHz is plotted against peak frequency of the relaxation oscillation, fr, for YbEr-DFB-2.

Figure 8 Response to a 5-cycle sine tone burst at 250 kHz.

(a) Voltage applied to PA-g, (b) output from PA-s, and (c) laser YbEr-DFB-2.

Figure 9 The laser YbEr-DFB-1 response to the impact of a steel ball of 0.43g dropped from a height of 7cm.

Figure 1

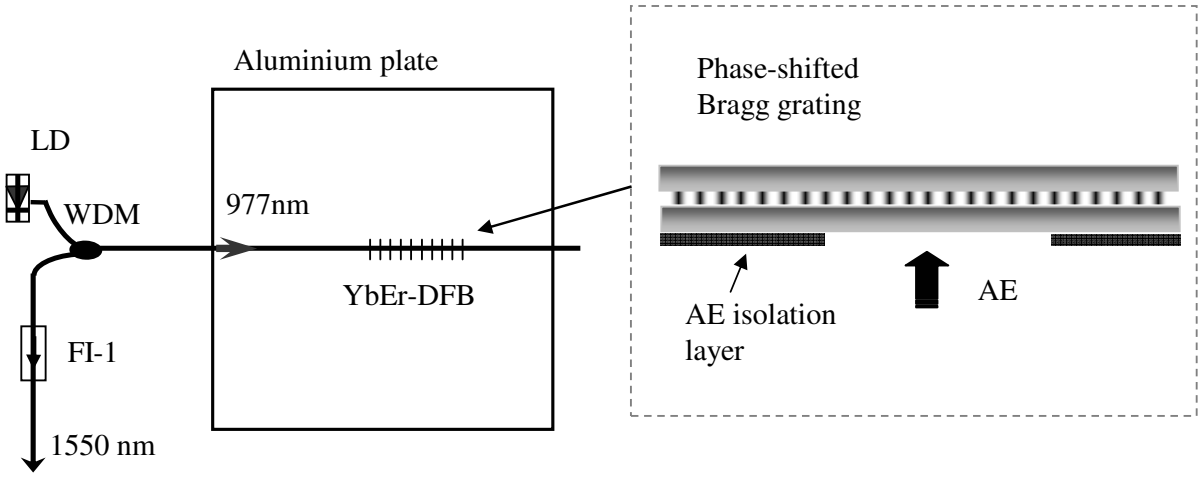
Aluminium plate
LD
WDM
977nm
YbEr-DFB
FI-1
1550 nm
Phase-shifted
Bragg grating
AE isolation
layer
AE

Figure 2

Figure 2 (a)

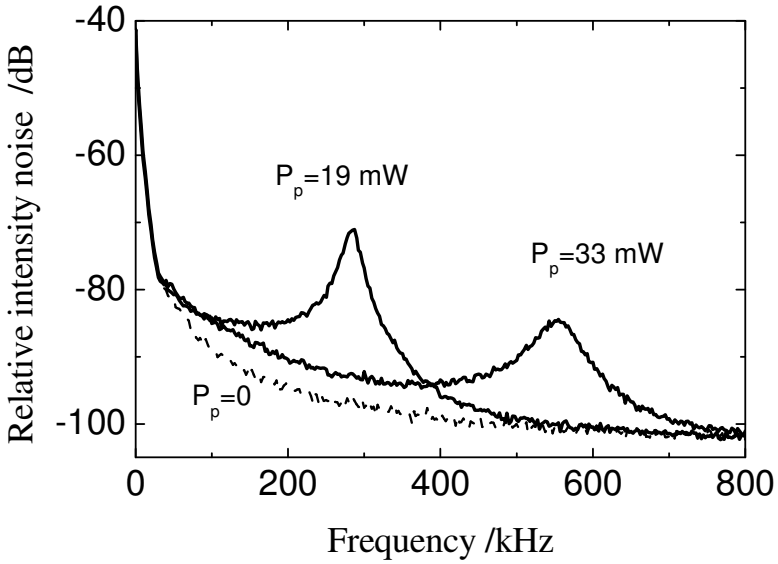

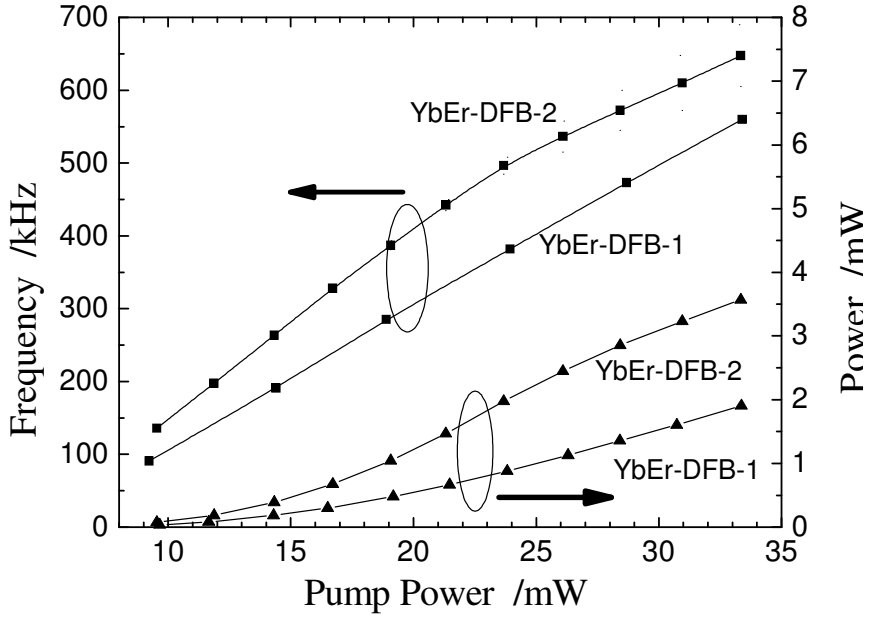

Figure 2 (b)

Figure 3

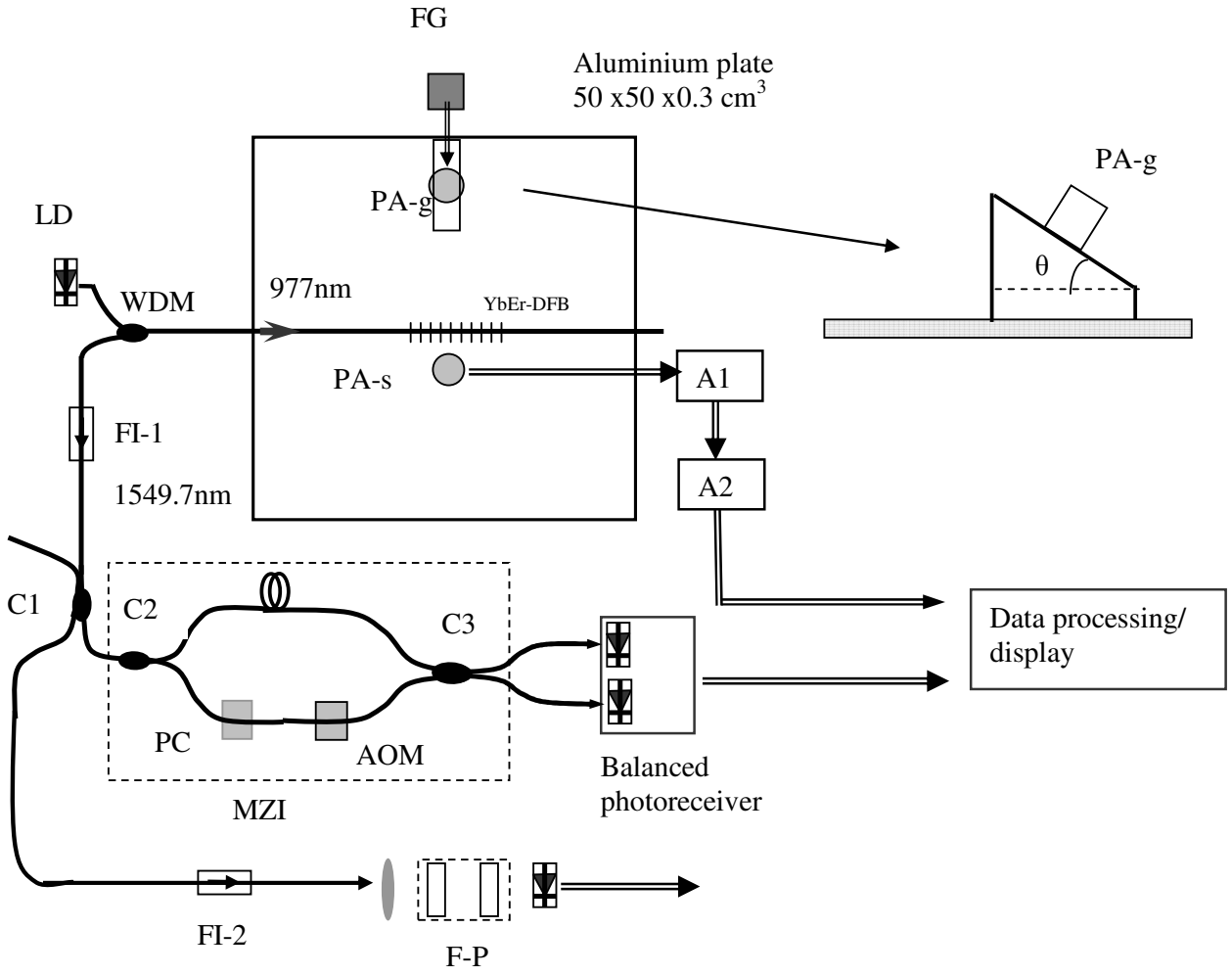
FG
Aluminium plate
50 x50 x0.3 cm3
PA-g
LD
WDM
977nm
YbEr-DFB
PA-s
A1
A2
FI-1
1549.7nm
C1
C2
C3
PC
AOM
MZI
Balanced
photoreceiver
Data processing/
display
FI-2
F-P
θ

Figure 4

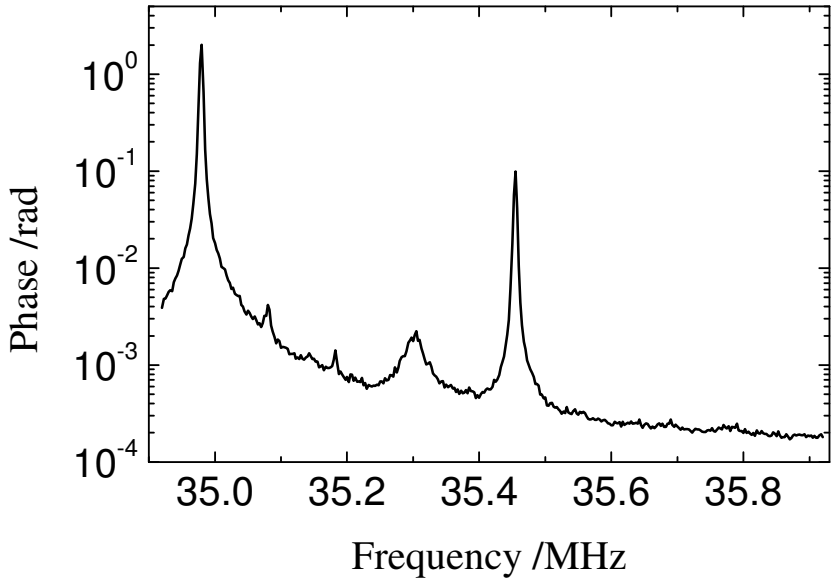
Phase /rad
10^0
10^-1
10^-2
10^-3
10^-4
35.0
35.2
35.4
35.6
35.8
Frequency /MHz

Figure 5

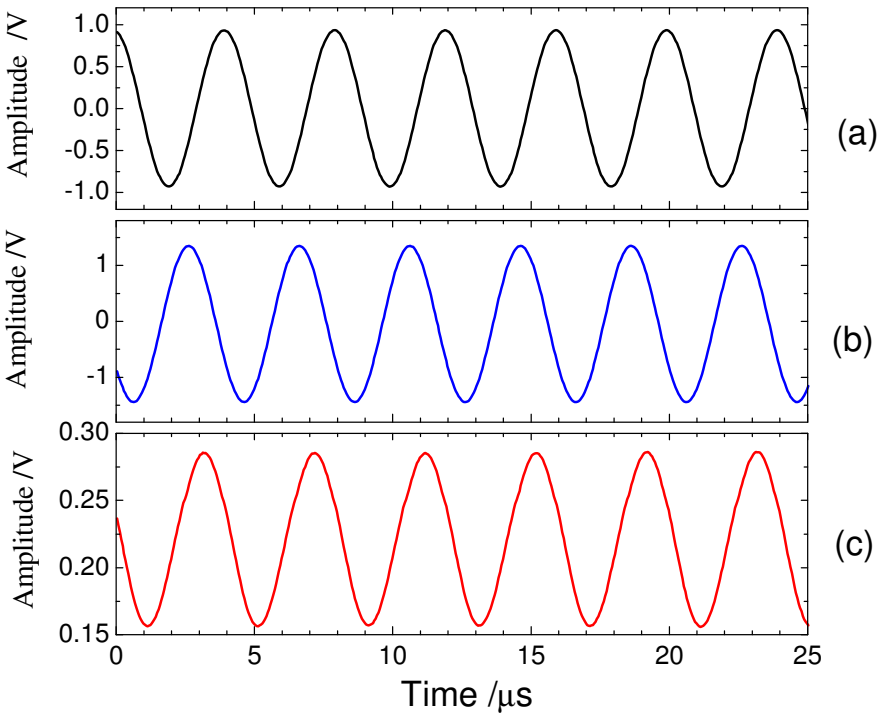
Amplitude /V
1.0
0.5
0.0
-0.5
-1.0
(a)
Amplitude /V
1
0
-1
(b)
Amplitude /V
0.30
0.25
0.20
0.15
(c)
0
5
10
15
20
25
Time /μs

Figure 6

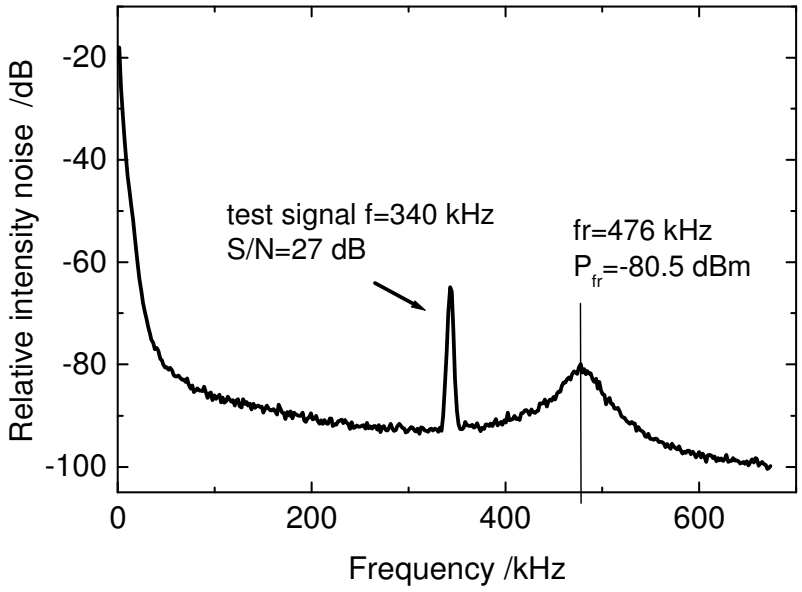

Figure 7

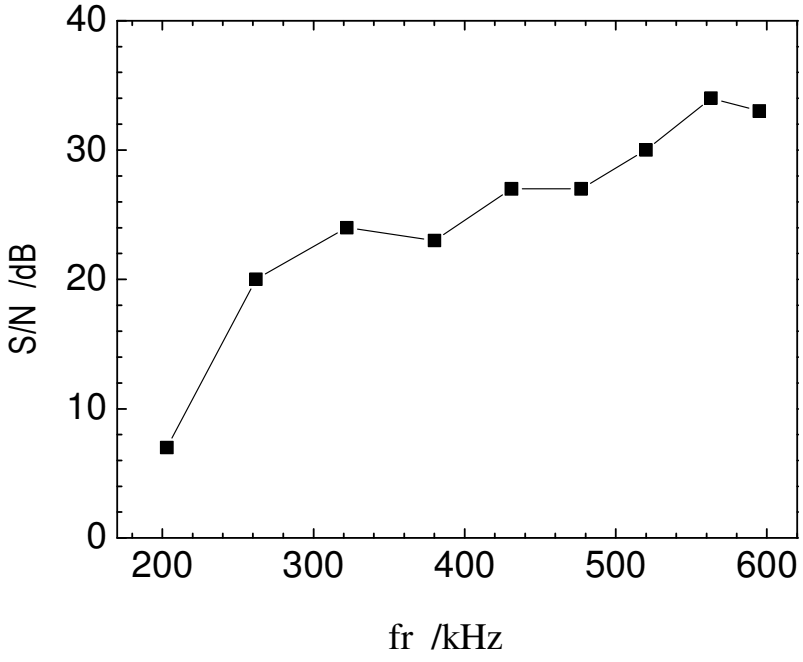

Figure 8

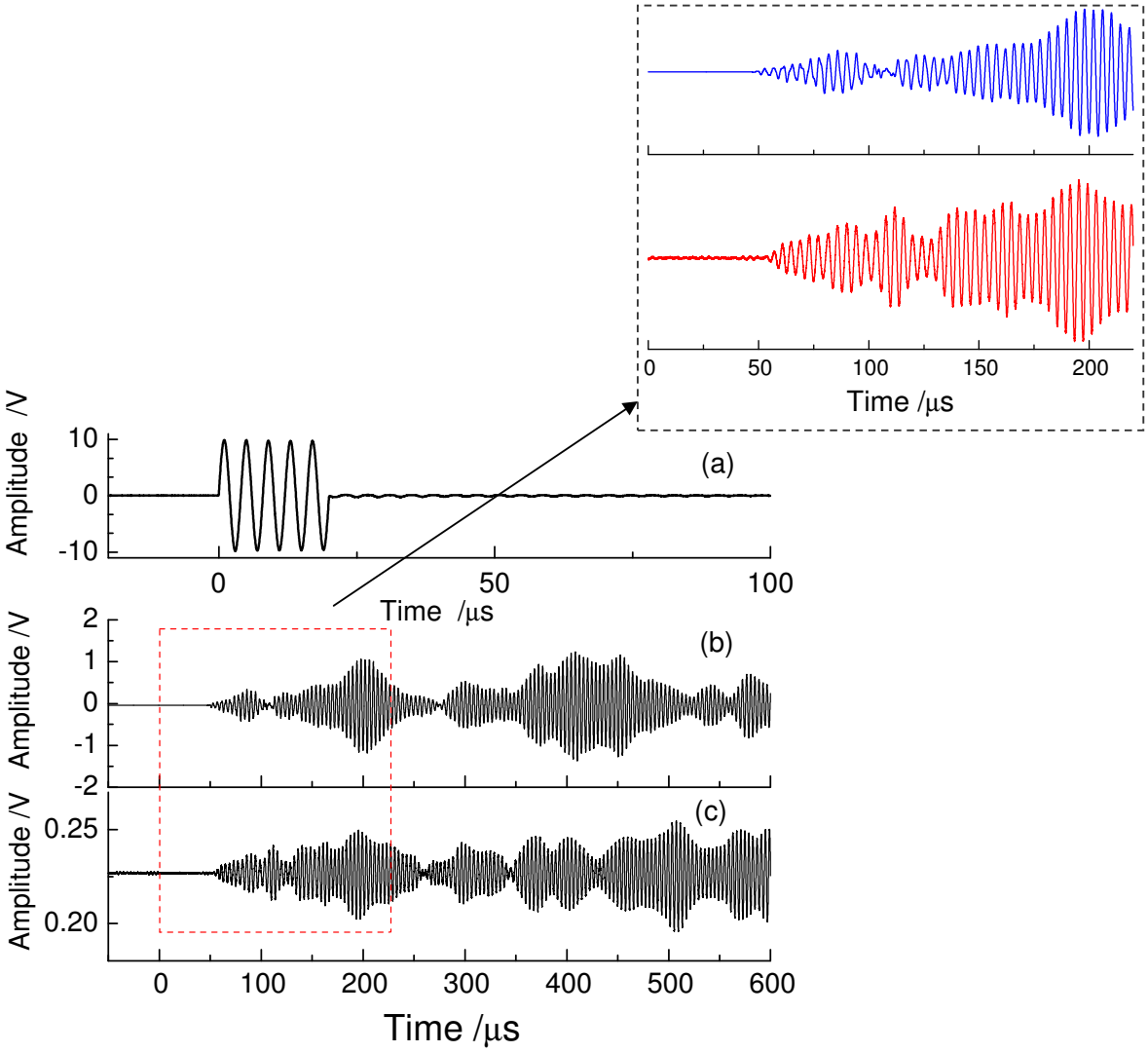
Amplitude /V
10
0
-10
0
50
100
Time /μs
(a)
0
50
100
150
200
Time /μs
Amplitude /V
2
1
0
-1
-2
(b)
Amplitude /V
0.25
0.20
(c)
0
100
200
300
400
500
600
Time /μs

Figure 9